



HAL
open science

Impact of propellers inertia and asymmetries on a V-shaped quadrotor

Gauthier Rousseau, Cristina Stoica Maniu, Sihem Tebbani, Mathieu Babel

► **To cite this version:**

Gauthier Rousseau, Cristina Stoica Maniu, Sihem Tebbani, Mathieu Babel. Impact of propellers inertia and asymmetries on a V-shaped quadrotor. Preprints of the 20th World Congress of the International Federation of Automatic Control, Jul 2017, Toulouse, France. pp.10686-10690. hal-01562854

HAL Id: hal-01562854

<https://hal.science/hal-01562854v1>

Submitted on 30 Aug 2019

HAL is a multi-disciplinary open access archive for the deposit and dissemination of scientific research documents, whether they are published or not. The documents may come from teaching and research institutions in France or abroad, or from public or private research centers.

L'archive ouverte pluridisciplinaire **HAL**, est destinée au dépôt et à la diffusion de documents scientifiques de niveau recherche, publiés ou non, émanant des établissements d'enseignement et de recherche français ou étrangers, des laboratoires publics ou privés.

Impact of Propellers Inertia and Asymmetries on a V-Shaped Quadrotor[★]

Gauthier Rousseau^{*,**} Cristina Stoica Maniu^{*}
Sihem Tebbani^{*} Mathieu Babel^{**}

^{*} *Laboratoire des Signaux et Systèmes, CentraleSupélec-CNRS-Univ. Paris-Sud, Université Paris Saclay, Gif-sur-Yvette, France*

(*e-mail: {gauthier.rousseau, cristina.stoica, sihem.tebbani}@supelec.fr*)

^{**} *Flight Control Department, Parrot Drones, Paris, France, (e-mail: {gauthier.rousseau, mathieu.babel}@parrot.com).*

Abstract: This paper emphasizes several dynamical aspects of a quadrotor induced by propellers inertia, especially when its rotors are tilted or asymmetrically distributed around its body. To achieve this, a simplified, linear model is established for a generic quadrotor and successively applied in three cases: a flat and symmetric quadrotor, a V-shaped quadrotor and finally an asymmetric quadrotor. The results are illustrated via numerical simulations.

Keywords: UAVs, quadrotors modelling.

1. INTRODUCTION

The use of quadrotors has dramatically increased during the last decade, with the rise of consumer quadrotors. These drones notably have applications in video making, but also in industries, such as construction sites management, agriculture monitoring or infrastructure inspection.

The most common quadrotor configuration is composed of four fan propellers, symmetrically disposed around the center of mass of the drone, alternating clockwise and anti-clockwise directions of rotation, and all pointing toward the vertical axis of the drone. This configuration is often referred to as an ‘X4’ configuration. The modelling and control of X4 quadrotors has been intensively studied, in such works as Shapovalov et al. (2014), Hamel et al. (2002), Bangura and Mahony (2014), Pounds et al. (2006), etc.

With four propellers to control their six degrees of freedom (DOF) of motion, quadrotors constitute underactuated systems. Consequently, these 6DOF cannot be controlled independently. Nevertheless, the actions of the propellers on the drone can be intuitively decoupled on an X4 quadrotor, which constitutes one advantage of this configuration.

However, with such a configuration, the dynamics on the yaw axis is usually inferior to those on the roll and pitch axes. This is due to the rotation around the yaw axis being mostly controlled using the propellers drag torques, while their lift is used for pitch and roll control, through the leverage it induces. Depending on the configuration, the latter tends to be 10 to 100 times stronger than the drag torques, resulting in weaker dynamics on the yaw axis.

A solution to balance these dynamics is to tilt the propellers axes in order to have a leverage induced by the lift on the yaw axis, too. This can be achieved by actuating the orientation of the propellers, as in Moutinho et al.

(2015), or by using non-X4 configurations. In Hossain et al. (2012), an Y4 (‘V-tail’) configuration is studied, with the rear propellers tilted in a ‘V’ shape. Studies on a Lynxmotion Hunter V400 frame, a popular V-tail frame among hobbyists, has also been lead recently in Bellocchio et al. (2016).

Furthermore, when adding payloads on the drone, the center of mass could be moved and the action of the different propellers could become asymmetric. Such an asymmetry can also be a matter of design, for instance, in order to achieve a better aerodynamic profile.

The main contribution of this paper consists in analyzing the effects of the propellers orientation and asymmetries on a V-shaped quadrotor. More specifically, we highlight a nonminimum phase behaviour on the pitch dynamics due to the action of propellers inertia, appearing when the V-angle increases. In addition, for asymmetrical drones, coupling terms can arise between the different axes.

Notation. In the sequel, s_x , c_x , and t_x are used to denote $\sin x$, $\cos x$, and $\tan x$, respectively.

2. QUADROTOR MODELLING

We consider the movement of a quadrotor equipped with four propellers in the inertial reference frame $\mathcal{R}_W = (O, \mathbf{x}_W, \mathbf{y}_W, \mathbf{z}_W)$. We choose $\mathcal{R}_B = (G, \mathbf{x}_B, \mathbf{y}_B, \mathbf{z}_B)$ as the body-fixed frame, with G the center of mass of the quadrotor (Fig. 1). We assume $\mathbf{z}_W = \mathbf{z}_B$ in case of hovering without perturbation. The quadrotor and its propellers are supposed to be rigid. The position of the center of mass in the inertial frame is given by $\mathbf{r} = x \mathbf{x}_W + y \mathbf{y}_W + z \mathbf{z}_W$, and its speed in the inertial frame is denoted by $\dot{\mathbf{r}} = \dot{x} \mathbf{x}_W + \dot{y} \mathbf{y}_W + \dot{z} \mathbf{z}_W = u \mathbf{x}_B + v \mathbf{y}_B + w \mathbf{z}_B$. We use Euler angles (φ, θ, ψ) - convention ZYX - to describe the attitude of the drone, and thus we define the rotation matrix R , between \mathcal{R}_W and \mathcal{R}_B

[★] The first author is a first year PhD student. This work was supported by Parrot Drones.

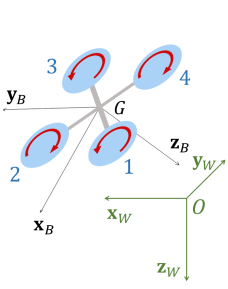


Fig. 1. Inertial & body-fixed frames

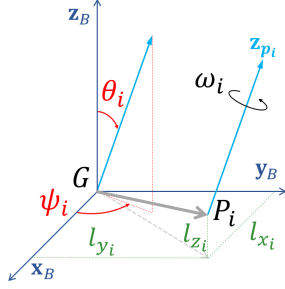


Fig. 2. Position & orientation of propeller i

$$\begin{pmatrix} \dot{x} \\ \dot{y} \\ \dot{z} \end{pmatrix} = \underbrace{\begin{pmatrix} c_\theta c_\psi & s_\varphi s_\theta c_\psi - c_\varphi s_\psi & c_\varphi s_\theta c_\psi + s_\varphi s_\psi \\ c_\theta s_\psi & s_\varphi s_\theta s_\psi + c_\varphi c_\psi & c_\varphi s_\theta s_\psi - s_\varphi c_\psi \\ -s_\theta & s_\varphi c_\theta & c_\varphi c_\theta \end{pmatrix}}_R \begin{pmatrix} u \\ v \\ w \end{pmatrix}$$

Denoting by $\boldsymbol{\Omega}_{B/W} = p \mathbf{x}_B + q \mathbf{y}_B + r \mathbf{z}_B$ the rotation speed vector of the drone in the inertial frame, the following expression holds

$$\begin{pmatrix} \dot{\varphi} \\ \dot{\theta} \\ \dot{\psi} \end{pmatrix} = \begin{pmatrix} 1 & s_\varphi t_\theta & c_\varphi t_\theta \\ 0 & c_\varphi & -s_\varphi \\ 0 & s_\varphi / c_\theta & c_\varphi / c_\theta \end{pmatrix} \begin{pmatrix} p \\ q \\ r \end{pmatrix} \quad (1)$$

For small φ and θ angles, (1) is equivalent to $(\dot{\varphi} \ \dot{\theta} \ \dot{\psi}) \approx (p \ q \ r)$. Finally, let m be the total mass of the quadrotor and $\mathbf{J} = \text{diag}(J_x, J_y, J_z)$ its inertia tensor in \mathcal{R}_B .

We will next consider the propellers, the gravity and the body drag influence in order to derive a linear model for the system dynamics near the hovering equilibrium.

Propellers. The drone is equipped with four propellers, (p_1, p_2, p_3, p_4) . Denoting by P_i the center of mass of the propeller p_i , its position in the body-fixed frame \mathcal{R}_B is $\overrightarrow{GP}_i = l_{x_i} \mathbf{x}_B + l_{y_i} \mathbf{y}_B + l_{z_i} \mathbf{z}_B$. The rotation speed vector of the propeller p_i in \mathcal{R}_B is $\boldsymbol{\Omega}_{p_i/B} = \omega_i \mathbf{z}_{p_i}$, with $\omega_i > 0$. The orientation of \mathbf{z}_{p_i} in \mathcal{R}_B is given by the angles $\psi_i \in [-\pi, \pi]$ and $\theta_i \in [0, \pi]$, as illustrated in Fig. 2, $\mathbf{z}_{p_i} = s_{\theta_i} c_{\psi_i} \mathbf{x}_W + s_{\theta_i} s_{\psi_i} \mathbf{y}_W + c_{\theta_i} \mathbf{z}_W$.

A quadratic model is chosen for the lift force \mathbf{T}_i and drag torque $\boldsymbol{\Gamma}_i$ applied on the i -th propeller

$$\mathbf{T}_i = \alpha_i \omega_i^2 \mathbf{z}_{p_i}, \quad \boldsymbol{\Gamma}_i = \beta_i \omega_i^2 \mathbf{z}_{p_i} \quad (2)$$

with $\alpha_i > 0$ or $\alpha_i < 0$ depending on the orientation of the propeller in \mathcal{R}_B , and $\beta_i < 0$. We can linearize (2) near the hovering equilibrium state by defining $\omega_i = \omega_{h_i} + \delta\omega_i$, with ω_{h_i} the rotation speed of the i -th propeller when hovering (without any perturbation such as wind or ground effect). This allows approaching

$$\mathbf{T}_i \cdot \mathbf{z}_{p_i} \approx T_{0_i} + a_i \delta\omega_i, \quad \boldsymbol{\Gamma}_i \cdot \mathbf{z}_{p_i} \approx \Gamma_{0_i} + b_i \delta\omega_i$$

with $T_{0_i} = \alpha_i \omega_{h_i}^2$, $a_i = 2\alpha_i \omega_{h_i}$, $\Gamma_{0_i} = \beta_i \omega_{h_i}^2$, $b_i = 2\beta_i \omega_{h_i}$. The leverage induced by propellers lift is then

$$\boldsymbol{\Gamma}_{l_i} = \overrightarrow{GP}_i \times \mathbf{T}_i$$

Let us denote by J_{p_i} the inertia of the i -th propeller with respect to its rotation axis \mathbf{z}_{p_i} . The reaction torque applied on the quadrotor via the i -th propeller is given by

$$\boldsymbol{\Gamma}_{r_i} = -J_{p_i} \dot{\omega}_i \mathbf{z}_{p_i}$$

We neglect the gyroscopic torques generated by the propellers, as they are much smaller than those induced by

the propellers drag and lift for small rotation speeds of the drone. Since the quadrotor has four propellers, the total force applied by the propellers on the drone is $\sum_{i=1}^4 \mathbf{T}_i$, and the total torque is $\sum_{i=1}^4 (\boldsymbol{\Gamma}_i + \boldsymbol{\Gamma}_{l_i} + \boldsymbol{\Gamma}_{r_i})$.

Gravity. The gravity action on the drone is modeled by a constant force $\mathbf{f}_g = mg \mathbf{z}_W$. For small angles, this expression becomes

$$\mathbf{f}_g \approx -mg\theta \mathbf{x}_B + mg\varphi \mathbf{y}_B + mg \mathbf{z}_B \quad (3)$$

Body drag. We can add a simplified linear model of the aerodynamic drag of the quadrotor body around the hovering equilibrium state, as the combination of a force \mathbf{f}_d and a torque $\boldsymbol{\tau}_d$, given by

$$\mathbf{f}_d = -C_x u \mathbf{x}_B - C_y v \mathbf{y}_B - C_z w \mathbf{z}_B$$

$$\boldsymbol{\tau}_d = -C_p p \mathbf{x}_B - C_q q \mathbf{y}_B - C_r r \mathbf{z}_B$$

Thus, with small but constant angles, the drone model reaches a terminal velocity instead of accelerating indefinitely. Close to the hovering equilibrium, the action of body drag torques is reduced, since the rotation speed of the drone is supposed to be small anyway.

Linear Model. Applying the fundamental principle of dynamics leads to

$$\begin{aligned} m\ddot{\mathbf{r}} &= \mathbf{f}_g + \mathbf{f}_d + \sum_{i=1}^4 \mathbf{T}_i \\ \mathbf{J}\dot{\boldsymbol{\Omega}}_{B/W} &= \boldsymbol{\tau}_d + \sum_{i=1}^4 (\boldsymbol{\Gamma}_i + \boldsymbol{\Gamma}_{l_i} + \boldsymbol{\Gamma}_{r_i}) - \boldsymbol{\Omega}_{B/W} \times \mathbf{J}\boldsymbol{\Omega}_{B/W} \end{aligned} \quad (4)$$

At the hovering equilibrium, with (3), the following expression holds

$$\begin{aligned} \mathbf{0} &= mg \mathbf{z}_B + \sum_{i=1}^4 T_{0_i} \mathbf{z}_{p_i} \\ \mathbf{0} &= \sum_{i=1}^4 \Gamma_{0_i} \mathbf{z}_{p_i} \end{aligned} \quad (5)$$

For small angular speeds of the quadrotor, the expression (4) can be linearized by neglecting the term $\boldsymbol{\Omega}_{B/W} \times \mathbf{J}\boldsymbol{\Omega}_{B/W}$. Using (5), it comes

$$\begin{aligned} m\dot{u} &= -mg\theta - C_x u + u_u & J_x \dot{p} &= -C_p p + u_p \\ m\dot{v} &= mg\varphi - C_y v + u_v & J_y \dot{q} &= -C_q q + u_q \\ m\dot{w} &= -C_z w + u_w & J_z \dot{r} &= -C_r r + u_r \end{aligned} \quad (6)$$

where $(u_u \ u_v \ u_w \ u_p \ u_q \ u_r)^\top = B_{\omega \rightarrow u} \cdot (\delta\omega_1 \ \delta\omega_2 \ \delta\omega_3 \ \delta\omega_4)^\top + B_{\dot{\omega} \rightarrow u} \cdot (\delta\dot{\omega}_1 \ \delta\dot{\omega}_2 \ \delta\dot{\omega}_3 \ \delta\dot{\omega}_4)^\top$, with $B_{\omega \rightarrow u} = (B_1 \ B_2 \ B_3 \ B_4)$, $B_{\dot{\omega} \rightarrow u} = (B_{.1} \ B_{.2} \ B_{.3} \ B_{.4})$, and

$$B_i = \begin{pmatrix} a_i s_{\theta_i} c_{\psi_i} \\ a_i s_{\theta_i} s_{\psi_i} \\ a_i c_{\theta_i} \\ b_i s_{\theta_i} c_{\psi_i} + a_i (l_{y_i} c_{\theta_i} - l_{z_i} s_{\theta_i} s_{\psi_i}) \\ b_i s_{\theta_i} s_{\psi_i} + a_i (l_{z_i} s_{\theta_i} c_{\psi_i} - l_{x_i} c_{\theta_i}) \\ b_i c_{\theta_i} + a_i s_{\theta_i} (l_{x_i} s_{\psi_i} - l_{y_i} c_{\psi_i}) \end{pmatrix}, \quad B_{.i} = \begin{pmatrix} 0 \\ 0 \\ 0 \\ -J_{p_i} s_{\theta_i} c_{\psi_i} \\ -J_{p_i} s_{\theta_i} s_{\psi_i} \\ -J_{p_i} c_{\theta_i} \end{pmatrix} \quad (7)$$

Ideally, each of the 6DOF of the quadrotor would be decoupled and controlled independently. However, with only 4 propellers, the drone is underactuated and this is not possible. Nevertheless, it is usually possible to decouple the action of the propellers on the three rotation axes and the z translation axis. In this context, let us define the 4×4 *mixing matrix*

$$B_{\omega \rightarrow v} = (\mathbf{0}_{4,2} \ \mathbf{I}_4) B_{\omega \rightarrow u}$$

and its inverse, the *unmixing matrix*

$$B_{v \rightarrow \omega} = (B_{\omega \rightarrow v})^{-1}$$

A way to decouple w , p , q , and r is to introduce the decoupled control signals $(v_w \ v_p \ v_q \ v_r)$ such as

$$(u_u \ u_v \ u_w \ u_p \ u_q \ u_r)^\top = B_{\omega \rightarrow u} \cdot B_{v \rightarrow \omega} \cdot (v_w \ v_p \ v_q \ v_r)^\top + B_{\dot{\omega} \rightarrow u} \cdot B_{v \rightarrow \omega} \cdot (\dot{v}_w \ \dot{v}_p \ \dot{v}_q \ \dot{v}_r)^\top$$

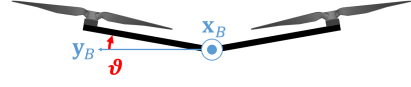


Fig. 3. A V-shaped quadrotor

3. X4 AND V4 CONFIGURATIONS

X4 Quadrotor. A quadrotor is in X4 configuration when its two plans $(G, \mathbf{x}_B, \mathbf{z}_B)$ and $(G, \mathbf{y}_B, \mathbf{z}_B)$ are symmetry plans and the 4 propellers are oriented toward $\pm \mathbf{z}_B$. For an X4 configuration as shown on Fig. 1, we typically have the following values for the system parameters

$$\begin{pmatrix} \psi_1 & \theta_1 & l_{x1} & l_{y1} & l_{z1} & a_1 & b_1 & J_{p1} \\ \psi_2 & \theta_2 & l_{x2} & l_{y2} & l_{z2} & a_2 & b_2 & J_{p2} \\ \psi_3 & \theta_3 & l_{x3} & l_{y3} & l_{z3} & a_3 & b_3 & J_{p3} \\ \psi_4 & \theta_4 & l_{x4} & l_{y4} & l_{z4} & a_4 & b_4 & J_{p4} \end{pmatrix} = \begin{pmatrix} 0 & \pi & l_x & -l_y & 0 & a & -b & J_p \\ 0 & 0 & l_x & l_y & 0 & -a & -b & J_p \\ 0 & \pi & -l_x & l_y & 0 & a & -b & J_p \\ 0 & 0 & -l_x & -l_y & 0 & -a & -b & J_p \end{pmatrix} \quad (8)$$

with $l_x > 0$, $l_y > 0$, $a > 0$, and $b > 0$. We then find the usual expressions

$$B_{\omega \rightarrow u} = \begin{pmatrix} 0 & 0 & 0 & 0 \\ 0 & 0 & 0 & 0 \\ -a & -a & -a & -a \\ l_y a & -l_y a & -l_y a & l_y a \\ l_x a & l_x a & -l_x a & -l_x a \\ b & -b & b & -b \end{pmatrix}, B_{\dot{\omega} \rightarrow u} = \begin{pmatrix} 0 & 0 & 0 & 0 \\ 0 & 0 & 0 & 0 \\ 0 & 0 & 0 & 0 \\ 0 & 0 & 0 & 0 \\ J_p & -J_p & J_p & -J_p \end{pmatrix}$$

The propellers action on the x and y translation axes are null and their action on the z translation axis and the three rotation axes can be fully decoupled: $B_{\omega \rightarrow u} \cdot B_{v \rightarrow \omega} = \begin{pmatrix} \mathbf{0}_{2,4} \\ \mathbf{I}_4 \end{pmatrix}$, $B_{\dot{\omega} \rightarrow u} \cdot B_{v \rightarrow \omega} = \begin{pmatrix} \mathbf{0}_{5,3} & \mathbf{0}_{5,1} \\ \mathbf{0}_{1,3} & \frac{J_p}{b} \end{pmatrix}$. Then, we can write

$$\begin{aligned} u_u(s) &= 0, & u_v(s) &= 0, & u_w(s) &= v_w(s), \\ u_p(s) &= v_p(s), & u_q(s) &= v_q(s), & u_r(s) &= \left(1 + \frac{J_p}{b} s\right) v_r(s), \end{aligned} \quad (9)$$

with s the Laplace variable. To simplify the notation, the dependence on the s variable of the input/output signals is further omitted. Finally, using (6) and (9), we can write the following transfer functions

$$\begin{aligned} u &= \frac{-mg}{s(C_q + J_y s)(C_x + m s)} v_q, & w &= \frac{1}{C_z + m s} v_w, \\ v &= \frac{mg}{s(C_p + J_x s)(C_y + m s)} v_p, & r &= \frac{1 + \frac{J_p}{b} s}{C_r + J_z s} v_r \end{aligned}$$

Propellers inertia induces a zero in the yaw dynamics. The latter is usually significant, and allows us to reduce and to smooth the control signals on this axis during dynamic flight phases.

V4 Quadrotor. On an X4 configuration, the yaw axis is controlled using the propellers drag and the reaction torques. These tend to be one or more orders of magnitude inferior to the torques induced by the propellers lift on the roll and pitch axes. One way to improve a quadrotor dynamics on its yaw axis is then to tilt its propellers in a V-shape, as illustrated on Fig. 3. Sometimes only the rear propellers are tilted (called a V-Tail or Y4 configuration). In the present paper, we suppose that all the four propellers are tilted the same way (V4 configuration). In this context, we choose the same parameters as (8) with the difference $(\psi_1 \ \psi_2 \ \psi_3 \ \psi_4) = (\frac{\pi}{2} \ \frac{\pi}{2} \ -\frac{\pi}{2} \ -\frac{\pi}{2})$, $(\theta_1 \ \theta_2 \ \theta_3 \ \theta_4) = (\pi - \vartheta \ \vartheta \ \pi - \vartheta \ \vartheta)$ and $(l_{z1} \ l_{z2} \ l_{z3} \ l_{z4}) = (l_z \ l_z \ l_z \ l_z)$, with $\vartheta \in [0, \frac{\pi}{2}]$.

Such a configuration leads to

$$B_{\omega \rightarrow u} = \begin{pmatrix} 0 & 0 & 0 & 0 \\ a s_\vartheta & -a s_\vartheta & -a s_\vartheta & a s_\vartheta \\ -a c_\vartheta & -a c_\vartheta & -a c_\vartheta & -a c_\vartheta \\ a(l_y c_\vartheta - l_z s_\vartheta) & -a(l_y c_\vartheta - l_z s_\vartheta) & -a(l_y c_\vartheta - l_z s_\vartheta) & a(l_y c_\vartheta - l_z s_\vartheta) \\ -b s_\vartheta + a l_x c_\vartheta & -b s_\vartheta + a l_x c_\vartheta & b s_\vartheta - a l_x c_\vartheta & b s_\vartheta - a l_x c_\vartheta \\ b c_\vartheta + a l_x s_\vartheta & -b c_\vartheta - a l_x s_\vartheta & b c_\vartheta + a l_x s_\vartheta & -b c_\vartheta - a l_x s_\vartheta \end{pmatrix}$$

A part of the propellers lift is now added to their drag torques on the yaw axis, improving the dynamics of the drone on this axis. However, these drag torques also appear on the pitch axis now, and counter a part of the propellers lift, degrading the dynamics on this axis.

Inverting the rotation direction of each propeller (by changing the angles ψ_i and θ_i) leads to

$$B_{\omega \rightarrow u} = \begin{pmatrix} 0 & 0 & 0 & 0 \\ a s_\vartheta & -a s_\vartheta & -a s_\vartheta & a s_\vartheta \\ -a c_\vartheta & -a c_\vartheta & -a c_\vartheta & -a c_\vartheta \\ a(l_y c_\vartheta - l_z s_\vartheta) & -a(l_y c_\vartheta - l_z s_\vartheta) & -a(l_y c_\vartheta - l_z s_\vartheta) & a(l_y c_\vartheta - l_z s_\vartheta) \\ b s_\vartheta + a l_x c_\vartheta & b s_\vartheta + a l_x c_\vartheta & -b s_\vartheta - a l_x c_\vartheta & -b s_\vartheta - a l_x c_\vartheta \\ -b c_\vartheta + a l_x s_\vartheta & b c_\vartheta - a l_x s_\vartheta & -b c_\vartheta + a l_x s_\vartheta & b c_\vartheta - a l_x s_\vartheta \end{pmatrix}$$

The propellers lift now counters the propellers drag on the yaw axis, degrading the yaw dynamics. Since the propellers have been tilted in order to increase the yaw dynamics, this solution is not pertinent here. For this reason, hereafter, we will keep the directions of rotation as shown on Fig. 1 for the propellers.

Using the expressions

$$\begin{aligned} B_{\omega \rightarrow u} \cdot B_{v \rightarrow \omega} &= \begin{pmatrix} 0 & 0 & 0 & 0 \\ 0 & K_{pv} & 0 & 0 \\ \dots & \dots & \dots & \dots \\ \mathbf{I}_4 & & & \end{pmatrix} \\ B_{\dot{\omega} \rightarrow u} \cdot B_{v \rightarrow \omega} &= \begin{pmatrix} \dots & \dots & \dots & \dots \\ \dots & \mathbf{0}_{4,4} & \dots & \dots \\ 0 & 0 & \tau_q & 0 \\ 0 & 0 & 0 & \tau_r \end{pmatrix} \end{aligned} \quad (10)$$

with $K_{pv} = \frac{s_\vartheta}{l_y c_\vartheta - l_z s_\vartheta}$, $\tau_q = \frac{J_p s_\vartheta}{b s_\vartheta - a l_x c_\vartheta}$, $\tau_r = \frac{J_p c_\vartheta}{b c_\vartheta + a l_x s_\vartheta}$, the following transfer functions are obtained

$$\begin{aligned} u_u &= 0, & u_v &= K_{pv} v_p, & u_w &= v_w, \\ u_p &= v_p, & u_q &= (1 + \tau_q s) v_q, & u_r &= (1 + \tau_r s) v_r \end{aligned}$$

The differences with respect to (9) are the following: u_v and u_p are now coupled and a zero appears on the pitch axis, as a part of the torques induced by the propeller inertia. For realistic ϑ angles and a , b , and l_x coefficients, the propellers lift action on the pitch axis is still much stronger than the action of the propellers drag torques, and $b s_\vartheta < a l_x c_\vartheta$. This zero on the pitch axis is usually a positive real scalar, inducing a nonminimum phase behaviour on the pitch axis. However, this is usually a high frequency zero that only affects the very beginning of the transient response of the pitch axis (see Section. 4).

Finally, using (6), we can write the next transfer functions

$$\begin{aligned} u &= \frac{-mg}{s(C_q + J_y s)(C_x + m s)} v_q, & w &= \frac{1}{C_z + m s} v_w, \\ v &= \frac{mg + K_{pv} C_p s + K_{pv} J_x s^2}{s(C_p + J_x s)(C_y + m s)} v_p, & r &= \frac{1 + \tau_r s}{C_r + J_z s} v_r \end{aligned}$$

It can be noticed that zeros are introduced in the transfer functions of the speeds u and v , in comparison to the X4 configuration.

Asymmetrical Quadrotor. Due to payloads, aerodynamic design or other reasons, industrial quadrotors can have asymmetric configurations. For instance, the distance $\|\overrightarrow{GP_i}\|$ can differ from one propeller to another, or the propellers themselves can be different. We study here a drone which has a front/back asymmetry, but the same reasoning can be applied to other configurations. The difference with (8) is (uperscript f for front, b for back)

$$\begin{pmatrix} l_{x1} & l_{y1} & a_1 & b_1 & J_{p1} \\ l_{x2} & l_{y2} & a_2 & b_2 & J_{p2} \\ l_{x3} & l_{y3} & a_3 & b_3 & J_{p3} \\ l_{x4} & l_{y4} & a_4 & b_4 & J_{p4} \end{pmatrix} = \begin{pmatrix} l_x^f & -l_y^f & a^f & -b^f & J_p^f \\ l_x^f & l_y^f & -a^f & -b^f & J_p^f \\ -l_x^b & l_y^b & a^b & -b^b & J_p^b \\ -l_x^b & -l_y^b & -a^b & -b^b & J_p^b \end{pmatrix} \quad (11)$$

Such a configuration leads to

$$B_{\omega \rightarrow u} \cdot B_{v \rightarrow \omega} = \begin{pmatrix} \mathbf{0}_{2,4} \\ \mathbf{I}_4 \end{pmatrix}$$

$$B_{\dot{\omega} \rightarrow u} \cdot B_{v \rightarrow \omega} = \begin{pmatrix} \dots & \mathbf{0}_{5,4} & \dots \\ 0 & \tau_{pr} & 0 & \tau_{rr} \end{pmatrix}$$

with $\tau_{pr} = \frac{b^b J_p^f - b^f J_p^b}{a^f b^b l_y^f + a^b b^f l_y^b}$, $\tau_{rr} = \frac{a^f l_y^f J_p^b + a^b l_y^b J_p^f}{a^f b^b l_y^f + a^b b^f l_y^b}$. Depending on the configuration, propellers inertia can now couple the roll and yaw axes during dynamic flight phases, i.e.

$$u_w = v_w, \quad u_p = v_p, \quad u_q = v_q,$$

$$u_r = (1 + \tau_{rr} s) v_r + \tau_{pr} s v_p$$

For the same set of parameters as in (11), with the difference $(\psi_1 \psi_2 \psi_3 \psi_4) = (\frac{\pi}{2} \frac{\pi}{2} - \frac{\pi}{2} - \frac{\pi}{2})$, $(\theta_1 \theta_2 \theta_3 \theta_4) = (\pi - \vartheta^f \vartheta^f \pi - \vartheta^b \vartheta^b)$, $(l_{z1} l_{z2} l_{z3} l_{z4}) = (l_z^f l_z^f l_z^b l_z^b)$, i.e. a V-shaped quadrotor with front/back asymmetries, we can show that

$$B_{\omega \rightarrow u} \cdot B_{v \rightarrow \omega} = \begin{pmatrix} 0 & 0 & 0 & 0 \\ 0 & K_{pv} & 0 & K_{rv} \\ \dots & \dots & \mathbf{I}_4 & \dots \\ \dots & \dots & \mathbf{0}_{4,4} & \dots \end{pmatrix} \quad (12)$$

$$B_{\dot{\omega} \rightarrow u} \cdot B_{v \rightarrow \omega} = \begin{pmatrix} \dots & \dots & \dots & \dots \\ \tau_{wq} & 0 & \tau_{qq} & 0 \\ 0 & \tau_{pr} & 0 & \tau_{rr} \end{pmatrix}$$

with K_{pv} , K_{rv} , τ_{wq} , τ_{pr} having a null/positive/negative value, depending on the configuration, τ_{qq} usually negative as previously seen and inducing a positive zero in the pitch dynamics, and τ_{rr} usually positive. This leads to

$$u_v = K_{pv} v_p + K_{rv} v_r, \quad u_w = v_w, \quad u_p = v_p,$$

$$u_q = (1 + \tau_{qq} s) v_q + \tau_{wq} s v_w,$$

$$u_r = (1 + \tau_{rr} s) v_r + \tau_{pr} s v_p$$

The transfer functions of the linearized model (6) become

$$u = -mg \frac{1}{(C_q + J_y s)(C_x + m s)} \left(\frac{(1 + \tau_{qq} s)}{s} v_q - \tau_{wq} v_w \right)$$

$$v = \frac{mg + K_{pv} C_p s + K_{rv} J_x s^2}{s(C_p + J_x s)(C_y + m s)} v_p + \frac{K_{rv}}{C_y + m s} v_r$$

$$w = \frac{1}{C_z + m s} v_w, \quad r = \frac{1 + \tau_{rr} s}{C_r + J_z s} v_r + \frac{\tau_{pr} s}{C_r + J_z s} v_p$$

The front/back asymmetry can then couple the roll and yaw dynamics, and the pitch and vertical acceleration dynamics. Up to two additional zeros can be introduced in the pitch and yaw dynamics depending on the configuration. These real zeros can be positive or negative, depending on the configuration.

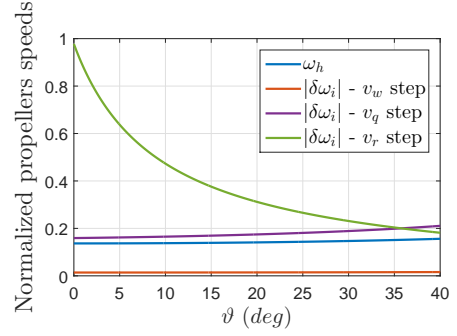


Fig. 4. Propellers speed at the hovering equilibrium state ω_h , and steady state propellers speed control signals $\delta\omega_i$ in response to v_w , v_q , and v_r steps, for different V angles of a given symmetric V4 quadrotor.

4. SIMULATION RESULTS

Motor model. For the following simulation study, each brushless motor is controlled by a rotation speed controller which is assumed to confer the motors a second order low-pass filter behaviour near the hovering equilibrium state

$$\delta\ddot{\omega}_i + 2\xi_i\omega_{0_i} \delta\dot{\omega}_i + \omega_{0_i}^2 \delta\omega_i = \omega_{0_i}^2 u_{\omega_i}$$

We also assume that the control law is designed to give the same dynamics to each motor, regardless the asymmetry of the drone. For the following simulations, these second order filters have a damping factor ξ_i close to 1.

Case 1: V4 quadrotor simulation. A simulation of the linear model was performed for a symmetric quadrotor in V4 configuration, for different values of the V-angle ϑ , and with a realistic set of parameters (mass, inertia, thrust and drag coefficients, $\|\overrightarrow{GP_i}\|$ distances). For a V-angle of 10° on each propeller, the required propellers rotation speeds $\delta\omega_i$ to achieve a given torque on the yaw axis was divided by two in steady state (see Fig. 4). In the mean time, those required to obtain a given torque on the pitch axis and a given force on the z axis were nearly unchanged (less than 5% higher), up to a ϑ angle of 20° ($\sim 10\%$ higher).

Fig. 5 shows the evolution of the total propellers torque on the pitch axis u_q in response to a step of decoupled control torque v_q . The impact of the V-angle on a PID-controlled pitch angle closed-loop was also simulated. The PID controller was tuned for a 0° V-angle, and its robustness regarding the positive real zero introduced by the V-angle is presented Fig. 6. As expected, the bigger the V-angle ϑ , the stronger the nonminimum phase behaviour in the pitch dynamics. However, the step response of u_q/v_q typically reaches its minimum in less than 10ms (Fig. 5), and the overshoot increases by 20% for a 40° V-angle on Fig. 6, and could be reduced by retuning the PID controller. Hence, the nonminimum phase behavior on the pitch axis is hardly visible for an angle ϑ that could reasonably be encountered on a potential industrial quadrotor.

In the mean time, Fig. 7 illustrates that as ϑ increases, the impact of propellers inertia dramatically decreases on the yaw axis (\sim halved for $\vartheta = 20^\circ$). As a consequence, if the V4 configuration improves the static gain between propellers speeds and propellers torques on \mathbf{z}_B , it could degrade the bandwidth on the yaw axis.

The impact of the coupling gain K_{pv} in (10) is illustrated by Fig.8. The force generated by the term $mg\varphi$ (in blue solid line) behaves more or less as a double integrator regarding v_p (and does not depend on ϑ). The dashed red line stands for the evolution of the term $K_{pv}v_p$, consisting in a simple static gain. Only the motor dynamics remains (also present in the term $mg\varphi$), giving here a second order low-pass filter behavior. The red line represents the sum of these two terms, and can be compared to the blue line to emphasize the extra dynamics added by the term $K_{pv}v_p$ on the V4 configuration.

Consequently, for a quadrotor designed to achieve high velocities along \mathbf{x}_B , it could be more interesting to tilt the propellers around \mathbf{y}_B , instead of \mathbf{x}_B . This way, the roll dynamics would be degraded, leading to a nonminimum phase behaviour, in favour of a better yaw dynamics, while the pitch dynamics would have a slightly higher bandwidth due to a coupling term between v_q and u_u .

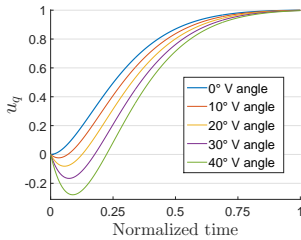


Fig. 5. $\frac{u_q}{v_q}$ step response

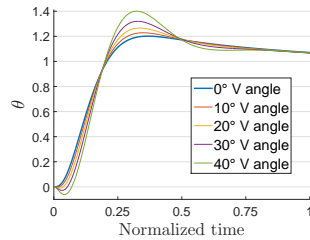


Fig. 6. $\frac{\theta}{\theta_{ref}}$ step response

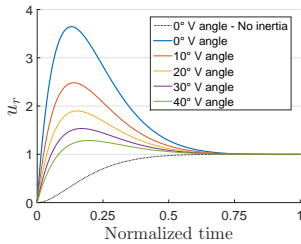


Fig. 7. $\frac{u_r}{v_r}$ step response

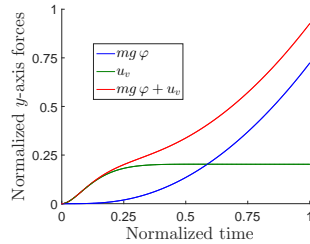


Fig. 8. V-shape impact on the y -axis

Case 2: Asymmetrical V-shaped quadrotor simulation. The model was also simulated in the case of V-shaped quadrotors containing front/back asymmetries. Several ‘realistic’ configurations were simulated, including a 3:1 ratio in terms of $\|\overrightarrow{GP}_i\|$ distances or propellers properties between the front and the back of the quadrotor, as well as V-tail configurations. The simulations confirmed the expected additional coupling terms brought by the asymmetries (see Section 5). However, their impact on the closed loop system was negligible most of the time. Only the term K_{rv} in (12) appeared significant for some V-tail configurations.

5. CONCLUSION

An X4 quadrotor can profit from propellers inertia to reduce and smooth yaw control signals during dynamic flight phases. However, using a simplified linear model of the quadrotor, we highlighted that, for a V-shape configuration, these inertia confer a nonminimum phase behaviour

to the pitch dynamics. This phenomenon may require caution for controllers stability on this axis. Nevertheless, simulations showed that for reasonable V angles, this behaviour can be neglected. Coupling terms were also highlighted when asymmetries arise between the propellers, especially in the case of V-tail configurations, for which yaw and lateral translation can be highly coupled.

In future work, a more profound study will be conducted on the nonlinear MIMO dynamics of the quadrotor, in order to better measure the impact of these coupling terms and additional zeros. Tests on a real system will be carried out in order to experimentally validate the results obtained in the simulation study.

In particular, far from the hovering equilibrium, not only the linearizations conducted Section 2 are not valid anymore, but much more complicated phenomena become significant. As described in Bristeau et al. (2009) or Huang et al. (2009), the propellers thrust can significantly deviate from their rotation axis due to aerodynamic effects. The drone body itself can also deform when experiencing high mechanical stress, modifying the orientation of the propellers.

In this context, there may be situations where, while the propellers are indeed oriented in a V-shape, their thrusts are not, or the effects of the V-shape become negligible regarding, for instance, other phenomena.

REFERENCES

- Bangura, M. and Mahony, R. (2014). Real-time model predictive control for quadrotors. In *19th IFAC World Congress*. South Africa, Cape Town.
- Bellocchio, E., Ciarfuglia, T.A., Crocetti, F., Ficola, A., and Valigi, P. (2016). Modelling and simulation of a quadrotor in V-tail configuration. *International Journal of Modelling, Identification and Control*, 26(2), 158–170.
- Bristeau, P.J., Martin, P., Salaün, E., and Petit, N. (2009). The role of propeller aerodynamics in the model of a quadrotor UAV. In *2009 European Control Conference (ECC)*, 683–688.
- Hamel, T., Mahony, R., Lozano, R., and Ostrowski, J. (2002). Dynamic modelling and configuration stabilization for an X4-flyer. In *15th IFAC World Congress*.
- Hossain, M.S., Kabir, A.M., Mazumder, P., Aziz, A., Hassan, M., Islam, M.A., and Saha, P.K. (2012). Design and development of an y4 copter control system. In *14th International Conference on Computer Modelling and Simulation (UKSim)*, 251–256.
- Huang, H., Hoffmann, G.M., Waslander, S.L., and Tomlin, C.J. (2009). Aerodynamics and control of autonomous quadrotor helicopters in aggressive maneuvering. *ICRA*.
- Moutinho, A., Mateos, E., and Cunha, F. (2015). The tilt-quadrotor: concept, modeling and identification. In *IEEE International Conference on Autonomous Robot Systems and Competitions*, 156–161. IEEE.
- Pounds, P., Mahony, R., and Corke, P. (2006). Modelling and control of a quad-rotor robot. *ACRA*.
- Shapovalov, I., Soloviev, V., Finaev, B.D., Zargaryan, J., and Kosenko, E. (2014). Research of the controlled flight dynamics based on the full and simplified quadrotor models. In *Advances in Engineering Mechanics and Materials*. Greece.